

國立交通大學

機械工程學系

碩士論文

Design and Implementation of Flip-Chip Mechanism

覆晶構裝機構之設計與實現



研究生：莊文彬

指導教授：成維華 教授

中華民國九十七年七月

覆晶構裝機構之設計與實現

研究生：莊文彬

Student : Wen-Pin Chuang

指導教授：成維華 教授

Advisor : Wei-Hua Chieng

國立交通大學

機械工程學系

碩士論文



A Thesis
Submitted to Institute of Mechanical Engineering
College of Engineering
National Chiao Tung University
in partial Fulfillment of the Requirements
for the Degree of
Master
In

Mechanical Engineering

July 2008

Hsinchu, Taiwan, Republic of China

中華民國九十七年七月

覆晶構裝機構之設計與實現

研究生：莊文彬

指導教授：成維華 教授

國立交通大學機械工程學系研究所

摘 要

由於封裝產業，不斷朝向 I/O 數高，體積縮小，系統整合，速度更快，及成本下降的趨勢。有鑒於目前台灣的設備自製率並不高，而關鍵零組件亦掌握在美，日，歐廠商手中，其中設備材料費用即佔了整體成本的六成以上，也使得封裝設備成本相對提高，本論文主旨在於發展設計覆晶設備中垂直定位系統與鍵合壓力控制。目前覆晶設備中，垂直定位與鍵合壓力控制方面大都以氣壓缸來驅動，但是氣壓會有滑跳效應使得鍵合壓力不易控制，因此本論文提出以伺服馬達定位加上以電磁力與彈簧力之制衡來做兩段式之垂直定位與壓力控制，並藉由編碼器和壓力感測器之量測數據作為此系統之回授訊號。

Design and Implementation of Flip-Chip Mechanism

Student : Wen-Pin Chuang

Advisor : Dr. Wei-Hua Chieng

Institute of Mechanical Engineering
National Chiao Tung University

Abstract

The Packaging industry continuously towards the plenty of I / O pins, size decreased, systems integration, faster, and cost down tendency. In view of Taiwan's current rate is not high self-made equipment, and critical Parts also held in the United States, Japan, and European manufacturers. The equipments and materials cost that account for more than 60 percent of the overall cost, and also make the packaging equipment costs relative increase. The main purpose of this thesis is to design the vertical positioning system and bonding force control of flip chip devices. Now, the vertical positioning system and bonding force control largely driven by pneumatic cylinder. But force control has the stick-slip effect makes bonding force difficult to control. Therefore, this thesis proposes to use two-stage control for vertical positioning and force control. The servomotor is for the Z-axis vertical positioning. And use the magnetic force and spring force to control the bonding force. The load cell and the encoder of servomotor are taken as the sensors of feedback signals in this system.

誌 謝

首先感謝我的指導老師 成維華 教授，在兩年的碩士生涯中給予我在學業及生活上的指導與教誨，並且從中得到了許多的啟發，相信在進入職場之後更能有自信的去面對及解決問題。

在這兩年裡，特別感謝楊嘉豐學長及吳秉霖學長的指導與建議，協助我在研究中解決問題讓我得以順利的完成論文，並且相當高興能認識學長們，學長們真的是「很厲害」。

在實驗室中，學長與學弟們也都相當好相處，也一起運動打球、聊天，舶強、奕旻、洋豪，跟你們一起在實驗室同甘共苦待了兩年，感謝洋豪的人腦火車時刻表、舶強的不用錢梨子吃到飽、奕旻的第一千金牙套，讓我這兩年的日子充滿歡樂，相信大家未來一定都有非常好的發展，大家「加油 好嗎?」。

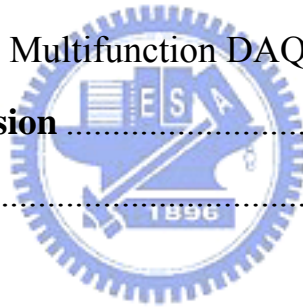
學弟們，冠今、安鎮、志隆、文祥、之浩，雖然跟你們宅的時間只有一年，但是也相當感謝你們在實驗室裡所帶來的歡樂，以及幫我輸入實驗數據的辛勞，不意外的話，希望你們都能順利畢業。

最後非常感謝我的父母支持我完成碩士學位，二十幾年來，你們總是不斷的鼓勵我、支持我，你們細心的照顧讓我在求學過程中無需擔心家裡或生活上的大小事，最後我沒有讓你們失望，終於完成了碩士學位。終於…畢業了。

Contents

摘要	i
Abstract	ii
誌謝	iii
Contents	iv
List of Figures	vi
List of Table	viii
Chapter 1 Introduction	1
1.1 Research Motives	1
1.2 Development of Flip Chip	2
1.3 Research Orientation	5
Chapter 2 Mechanism and Control System	6
2.1 Mechanism Design Conception	6
2.2 Mechanism Design Requirements	7
2.3 Mechanism Detail Illustration	7
2.3.1 Z-axis Vertical Positioning System	7
2.3.2 Force Control System	8
2.4 Motion Path Analysis and Planning	9
2.4.1 Z-axis Vertical Positioning Mechanism	9
2.4.2 Force Control Mechanism	10
2.5 Control System Architecture	10
2.5.1 Precision Positioning Introduction	11
2.5.2 Servomotor Close Loop Control	11
2.5.3 First Stage Z-axis Positioning	12
2.5.4 Second Stage Force Control	12

Chapter 3 Model of Force Control Mechanism	14
3.1 Ampere’s Law	15
3.2 Magnetic Circuit.....	16
3.3 The Force of Electromagnet.....	17
3.4 Bonding Force Control.....	19
3.4.1 Model of Force Control Mechanism	19
3.5 Experiment Result.....	22
Chapter 4 Hardware and Software Introduction	24
4.1 D.C. Servomotor	24
4.2 Load Cell	25
4.3 SMI Motor Control Software	25
4.4 NI USB-6229 Multifunction DAQ	26
Chapter 5 Conclusion	27
References	28



List of Figures

Figure 1.1 Pneumatic cylinder positioning system.	30
Figure 1.2 Lid closed.....	30
Figure 1.3 Six kinds of flip chip	31
Figure 2.1 Conceptual mechanism.....	31
Figure 2.2 conceptual force control mechanism.....	32
Figure 2.3 Fixed base and the four long-axis holes.	32
Figure 2.4 Timing pulley and timing belt.	33
Figure 2.5 Force control mechanism.	33
Figure 2.6 Relationship of position.....	34
Figure 2.7 The control system architecture.....	34
Figure 2.8 Servomotor close loop control.....	35
Figure 2.9 First stage positioning control block diagram.	35
Figure 2.10 Force control architecture.....	36
Figure 3.1 Coil around the square core.	36
Figure 3.2 Similarities of circuit and magnetic circuit.	37
Figure 3.3 magnetic circuit of force control mechanism.	37
Figure 3.4 Free state of force control mechanism.....	38
Figure 3.5 The free body diagram of force control mechanism, when it lifted up to bonding position.	38
Figure 3.6 Air gap =0mm, current=0.12A	39
Figure 3.7 Air gap =0.1mm, current=0.12A.	39
Figure 3.8 Air gap =0.2mm, current=0.12A.	40
Figure 3.9 Air gap=0.3mm, current=0.12A.	40
Figure 3.10 Air gap =0.4 mm, current=0.12A	41

Figure 3.11 Air gap =0.5 mm, current=0.12A	41
Figure 3.12 Air gap =0.6 mm, current=0.12A	42
Figure 3.13 Air gap =0.7 mm, current=0.12A	42
Figure 3.14 Air gap =0.8 mm, current=0.12A	43
Figure 3.15 Air gap=0.8mm,current=0.25A.	43
Figure 4.1 SmartMotor 2315D.....	44
Figure 4.2 FUTEK LSB200 10lb.....	44
Figure 4.3 SMI software.	45
Figure 4.4 NI USB-6229 DAQ card.	45



List of Table

Table 3.1 Duality of circuit and magnetic circuit. 46



Chapter 1 Introduction

1.1 Research Motives

In the current electronic, optoelectronic, communications, and other products, require high-power, high-calorie, high-planned, high memory capacity, high stability, in addition to the performance requirements of thin short, which IC packaging industry will derive various Packaging technology, With the rapid IC process Micro, the functions of IC lead to increased proliferation of IC-pin IC frequency and the enhancement of the electric transmission and cooling capacity requirements accordingly upgrade, this evolution can be achieved demand makes the "flip chip packaging technology" should be transported packaging industry to become a star. The information appliance (IA) the rise, the demand for portable electronic products surged, also causing meet the light, thin, short, small properties "chip size package (CSP; Chip Scale Package)" has become the trend. [1]

Flip Chip Packaging currently the most widely used metal bump of the bump and tin-lead bump, the bump 95% used in the LCD driver IC packaging, and the remaining 5 percent is used in the Smart Card products; tin Lead bump the scope of the application of a wide pan, a few feet from high to low number of IC both feet use, it could meet the high electric, high heat, high reliability and light, thin, short, small, and other functions, application of the products include computer products (eg, personal computers, handheld computers), communications products (eg, portable

phones, Internet products, launchers, base station), the automobile industry (eg, engine control devices, airbag control , ABS braking systems) and consumer products (eg, mobile video recorders, digital cameras, watches, flat panel display and IC card).

However, in flip chip bonding process, the substrate and wafer bonding force control is a big key, because the thin-chip bonding process resulted in the control of forces must be very careful, otherwise it will be very easy to chip cracking the information currently found, the bonding strength of the control agencies and actuators are pneumatic cylinder and hydraulic cylinder for the majority, as shown in Figure 1.1 and Figure 1.2, but due to pressure effects lead stick slip bonding strength of the control is very difficult, therefore This paper to design a two stage positioning and control system to control the strength bonding strength, improve chip yields.

1.2 Development of Flip Chip

Flip chip bonding for IBM was first developed in the 1960s. Its technology is in the grain of the metal pad solder bump formation, and formation in the base version of the solder bump and the relative grain of contact should be, and then the grain will be overturned at the base version will be on the tap all point junction. Flip Chip bonding with the shortest connection length, the best electrical characteristics, the maximum output/income tap density, and can reduce IC size and increase unit wafer production capacity.

Flip chip technology, also called "inverted crystal Packaging," or "inverted crystal Packaging Law" is a chip packaging technology. As

shown in Figure 1.3 This packaging technology is different from the last major chip package, the chip will be used to be placed on board (chip pad), and then a line technologies (wire bounding) will be on the chip and substrate link connecting point, and flip chip packaging technology is to connect point-bump, and then flip chip from the bump and substrate and gain a direct link.

Now flip chip technology has been widely used in microprocessor packaging, but also become graphics, special applications, and computer chip group, and other mainstream packaging technology, the market for flip chip technology with the thrust, Packaging industry must provide 8-inch and 12-inch wafer probe testing, bump growth, assembly, final test to the integrity of services.

The future of electronic products continued towards thin short, high-speed, high-pin number, and other features to the wire based on the traditional-style packaging will gradually NA, will be limited to the application of low/low-priced products. According to the investigation report IC Insights, logic IC products because of the increasingly complex functional requirements, the demand for pin-count packages, generally show an annual 12 percent to 13 percent increase rate. ASICs to high-end products as an example, in 2002 the highest pin-count requirements for 2100 feet, and is expected to 2007, the largest pin count will be as high as 3500 feet. The flip chip package in the coming trend, it was still will be moving a few feet high (I /O), fine pitch goal. In addition, the next addition to the demand for flip chip packaging equipment will continue to expand, flip chip testing equipment required for the development is also the focus of manufacturers. As Flip Chip Packaging internal use as electrical

bump-guided path, distribution of the entire chip, the chip center located in the vicinity of bump quality testing, also depends on the automatic detection equipment to ensure that bump quality, and as Flip Chip closure the tall installed several characteristics of single-chip probe up to 1000 pin over several of the vertical probe cards, will become test equipment manufacturers to compete for the potential of the market.

Flip Chip IC technology with the following main advantages:

- 1. Space more efficient:** the chip will be installed directly in the substrate can reduce the cost of space, both planar and thickness, Flip Chip can save a great deal of room. To replace the QFP IC Flip Chip, Chip area can be 900 mm² to 100 mm². More IO Contact: Flip Chip IC at the bottom of the entire chip for input / output connections, as can be installed at the bottom of the tap-tap than the more peripheral installation, Flip Chip IC can have more I / O contact.
- 2. Lines and wire bonding without:** Flip Chip IC chip will be installed directly in the substrate, the line can be avoided and wire bonding.
- 3. Flip Chip IC materials can be saved and more than QFP TAB IC.**
- 4. Heat consumption of the smaller and better heat dissipation** (because of shorter circuit), and can be installed in the back of the chip heat sinks, thermal conductivity closure glue or heat.
- 5. As Flip Chip IC welding points smaller, so its conductivity than QFP with the TAB IC better.** And Flip Chip IC to the shorter the distance between the substrate and chip directly, so its resistance and inductance extremely low. The signal response speed of the high-frequency components become faster and help greatly on operation in such as telecommunications equipment.

6. Flip Chip access is not legitimate to use fuse, there is no larger wire-bond in the junction of stress. Flip Chip is due to the use of direct welding, increased bonding strength.
7. Flip Chip for procedures than other patch technology faster, but can enhance joint reliability and cost savings.

1.3 Research Orientation

In this thesis, five of its chapter summarized as follows: The chapter 1 on flip chip technology for the development and application, then illustrate flip chip positioning system and force control system and the motives and objectives. Chapter 2 is mainly in the force control and positioning mechanism system to consider the design elements of movement and path planning. System design further detail parts and analysis and integration. Chapter 3 will introduce the principle of force control. And introduce the Ampere's law, magnetic circuit, force of electromagnet, magnetic reluctance. We will illustrate the model of force control mechanism, and control structure. Chapter 4 we will introduce the specifications and characteristics of DC servomotor, load cell and USB interface DAQ card. In chapter 5 we have a conclusion on our mechanism and experiment result.

Chapter 2 Mechanism and Control System

2.1 Mechanism Design Conception

Z-axis vertical positioning and force control are the two important keys of flip chip technology. So first using ball bearing screw rod, DC servo motor, precision linear shafts, timing pulley and timing belt to be the Z-axis positioning mechanism. And let electromagnet, the iron slab attracted by electromagnet, load cell, precise shaft, oil-less bearings and springs be the force control mechanism. And the force control mechanism is on a moveable platform that drives by the Z-axis positioning system. The conceptual z-axis positioning mechanism is shown in Figure 2.1. The first stage of Z-axis vertical positioning mechanism will lift the force control mechanism to the bonding position. The second stage is by controlling the magnetic force and spring force to change the bonding force. First, the springs are pre-compressed by the initial magnetic force. When we decrease the current of electromagnet slowly, at the same time the magnetic force between electromagnet and iron slab also decreases slowly. And when the magnetic force is less than spring force slowly, the iron slab that locked on the carrier platform will move up to increase the force between chip and substrate. So we can change the bonding force by current control. And in the middle of the flip chip mechanism have a load cell to measure the force between chip and substrate. The conceptual force control mechanism is shown in Figure 2.2.

2.2 Mechanism Design Requirements

Because Z-axis position control and force control are important in flip chip. So consider high precision and high stability is the primary mechanism design considerations. Usually reduce the weight and enhance actuation rigidity is the main countermeasure. Therefore should consider the following several requests before the design:[2]

1. The structure rigidity is high and the static dynamic characteristic has good performance.
2. Mechanism components are manufactured precision, make the system kinematic error to fall lowest.
3. The mechanism has high repetition in motion, and easy to compensate the motion error.
4. Low request for environment, and easy to operation.



2.3 Mechanism Detail Illustration

In this section will illustrate their capability and characteristic two parts of the mechanism. The following are two parts analysis:

2.3.1 Z-axis Vertical Positioning System

Z-axis vertical positioning mechanism system include DC servomotor, precise ball bearing screw, timing pulley and timing belt. First, the motor fixed base can fix the servomotor in addition also has four long-axis holes be drilled through in the corners. We can adjust the fixed base's position anytime by the four long-axis holes. This way can make the timing pulley

and timing belt is easier to assemble, and another important key is the fixed base can make the belt tight enough to avoid motion errors. On the base's shorter side also has a screw to lock the base again. See Figure 2.3. And the transmission system is using timing pulleys and timing belt. As shown in Figure 2.4. Using timing belt and timing pulley has many advantages. Example: Not easy to slide, the transmission system will not idle. When the servomotor drives the force control mechanism rise up by ball bearing screw at the same time the moveable platform also along the two precise linear slider upward smoothly. And the ball bearing screw is pre-compressed. For generally speaking, the goal of bearing pre-compression may induce as follows:[6,7]

- A. Increase the rigidity.
- B. Decrease the backlash and vibration.
- C. The processing precision is better.



2.3.2 Force Control System

In this mechanism, include springs, electromagnet, iron slab and load cell, oil-less bearings and precise shafts to be a force control mechanism system. As shown in Figure 2.5. The three springs are pre-compressed by the load and must keep an air gap about 4~5mm between iron slab and the electromagnet. So when we start the electromagnet, the springs could compress again by initial magnetic force and keep the iron slab that lock on the carrier platform contact with electromagnet. So we must consider the whole load to calculate the spring constant. And the second compression product with the spring constant is the output force when the magnetic

force is zero. In force control mechanism, when we decrease the current of electromagnet, the magnetic force would gradually less than spring force. So the carrier platform will move up by the oil-less bearing along the precise shafts. The oil-less bearing has advantages: low-noise, low-wear, high load...etc. We also change the gap between electromagnet and iron slab by a stack of papers, when the electromagnet has an initial current. Then the magnetic resistance will change for different air gap, and we can see the difference in the experiment results from load cell data curve.

2.4 Motion Path Analysis and Planning

From the foregoing mechanism can know that the movement is divided into two parts. The followings will illustrate the two stage movement paths.



2.4.1 Z-axis Vertical Positioning Mechanism

In the Z axis direction movement, considers to several kind positions of different need, therefore the following has several kind of positions.

A. Preparation position

This position is ready to bond the chip when we press the power button. And then the DC servo motor will lift the force control mechanism up to a position to execute the next commands.

B. Substrate placed position

This position is to place the substrate when the lid of chip is not covered. And this position is higher than the preparation position. So this higher position is easier to place the substrate.

C. Bonding position

When we place the substrate completely, the DC servo motor will lift up the moveable platform that bear the force control mechanism slowly to a position higher than substrate placed position. Then the substrate will touch the bonding chip that on the lid of chip chuck and keep a very small preload about 20g with each other. And the next step continuous by second stage of force control. The relationship of position is shown in Figure 2.6 [7,8]



2.4.2 Force Control Mechanism

When the force control mechanism lifted up to the bonding position and the next step is control the magnetic force between electromagnet and iron slab. We decrease the current of electromagnet step by step about 0.001A, the mechanism move up a small displacement and the load cell data will become larger until the value which we set. When they are contact with each other, the load cell will transmit the measured data, then we could control the magnetic force by the feedback signals.

2.5 Control System Architecture

In this thesis control system is divided into two parts. One is Z-axis positioning and the other is force control. And positioning control mode using the close loop D.C. servomotor. The close loop servomotor control of

the main considerations for its high response, high efficiency and positioning precision. Positioning system to meet demands by the closed loop servomotor control is because of the need to immediately reflect the current situation. The control system architecture is shown in Figure 2.7.

2.5.1 Precision Positioning Introduction

Motor power compared to hydraulic actuators and air compressor is easy to use. Its control, maintenance is better than hydraulic actuators and air compressor, but the output power less than hydraulic. Air actuator do not have a lot of power, but because not pollute the environment and been used. But it is not easy to do precision positioning. In positioning control, a common locator stepper motors, servomotors and linear servo motors. To meet the demands for precision positioning, the use of open loop stepper motor control the most simple and low cost, and the position of the use of high-resolution detector with servomotors, designers can easily reach the goal of high precision positioning. [9,10]

2.5.2 Servomotor Close Loop Control

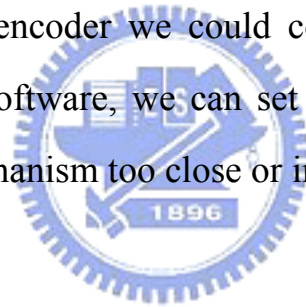
The positioning servo motor controller accept an order from the host computer (displacement and velocity), to compare the motor feedback signal of the position from position detection device. Through the position error after the operation through digital analog converter converted into an analog signal, sent to the motor driver. As shown in Figure 2.8. The use of servo motors advantages are as follows:[3, 4,5]

A. High speed response, and when low speed, sliding in smoothing.

- B. Choose the appropriate position sensors, can obtain the required accuracy of the servo system.
- C. High efficiency, low noise.

2.5.3 First Stage Z-axis Positioning

The first stage positioning control block diagram is shown in Figure 2.9. By the RS232, host computer and SMI motor control software, we can control the limit switch, rpm, or acceleration of SmartMotor. And by the inner encoder of SmartMotor we can know whether the position of servomotor out of step or not. If the position not in our demand, by the feedback signals of encoder we could compensate the position error. In SMI motor control software, we can set the software and hardware limit switch avoid the mechanism too close or impact.



2.5.4 Second Stage Force Control

The force control part is the second stage control when the first stage positioning finished. The second stage force control block diagram is a closed loop control, And force control architecture is shown in Figure 2.10 .When the force control mechanism lifted up to the bonding position, we can control the current of electromagnet from host computer and send the commands to the power supply by RS232. When chip and substrate bonding with each other, the load cell will transmit the feedback signals to the USB-6229 DAQ Card that we can see in computer. Then we can know whether the force too large or small than we set. If the force is less or more

than we set, the program will compensate or correct the bonding force by feedback signals.



Chapter 3 Model of Force Control Mechanism

Before we analyze the model, we define the physics meaning of each term in fundamental equation.

Nomenclature

H : Magnetic field intensity

l_c : Average length of path in the square core

I_{net} : Net current of integral loop through the magnetic field

N : Coil turns of electromagnet

i : Current in the coil

B : Magnetic flux density

μ : Magnetic permeability of material

F : Magnetomotive force

Φ : Magnetic field flux

R : Magnetic reluctance

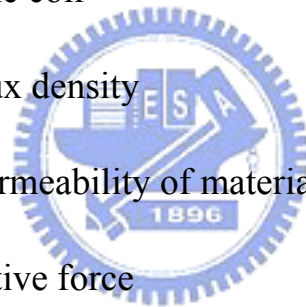
A : Area of cross section of magnetic circuit

U_B : Unit magnetic energy

μ_0 : Permeability of air

W_m : Magnetic energy

\hat{F} : Magnetic force



i_0 : Initial current of electromagnet

K_P : Spring constant of paper

K_L : Spring constant of load cell

K_S : Spring constant of spring

n : Numbers of paper

d : Thickness of paper

X_c : Compression of paper

X_S : Compression of spring

x : Displacement of iron slab



3.1 Ampere's Law

The current in the wire will form a magnetic field around the wire, its relationship as follows

$$\oint H \cdot dl_c = I_{net} \quad (3-1)$$

H is the magnetic field intensity, caused by the net current I_{net} , in units of ampere-turns/meter. We can use a coil around the square core as an example to illustrate Ampere's law. As shown in Figure 3.1. The core which is composed of magnetic material (ferromagnetic material) posed by the assumption that magnetic field (magnetic lines) caused by the current in the coil are all stay within the core. By Ampere's Law we can know l_c is

the average length of path in the square core, and I_{net} is equal to the net current of integral loop through the magnetic field, $N \cdot i$. As follows

$$H \cdot l_c = N \cdot i \quad (3-2)$$

And H is the magnetic field intensity

$$H = \frac{N \cdot i}{l_c} \quad (3-3)$$

From the magnetic field intensity, know the current in the coil is proportional to the number of circle, but inversely proportional to the length of magnetic circuit. Therefore, the average length of the larger magnetic circuit, the magnetic field intensity is smaller. Magnetic line is the amount of magnetic field flux, and the amount is related to the core of materials. And the amount of magnetic field flux can be magnetic flux density B , and its relations with magnetic field intensity.[11,12,13]

$$B = \mu H \quad (3-4)$$

3.2 Magnetic Circuit

In the circuit, the current flow path known as the circuit. In magnetic field, the magnetic field flux of space known as the magnetic circuit. The current in the circuit in the form of loop, just like the magnetic field flux in the magnetic circuit to form a loop. Current flows in the circuit, there must be a source of electromotive force. In the flow of magnetic flux in the magnetic circuit must also be a source of magnetomotive force. On the electric and magnetic terms of the duality, we can know the similarities in Figure 3.2 and Table 3.1. And the magnetic circuit, magnetomotive force as

follows

$$F = N \cdot i \quad (3-5)$$

And in the magnetic circuit, the relation of magnetomotive force with magnetic reluctance R is

$$F = \Phi \cdot R \quad (3-6)$$

Where, Φ is the magnetic field flux. From the Table 3.1 know as follows

$$R = \frac{l_c}{\mu A} \quad (3-7)$$

A is the cross-section area of the core.[11,12,14]

3.3 The Force of Electromagnet

Electromagnet is the kind of universal application of the magnets, because we can easily launch of its magnetic or eliminate. In our life we often use of magnetic energy and mechanical energy exchange to make the machine work. And in any magnetic field, any point in the space of magnetic energy density is defined as [12]

$$U_B = \frac{B^2}{2\mu_0} \quad (3-8)$$

In this thesis, the magnetic energy saving between electromagnet and iron slab can be expressed with follows

$$W_m = \frac{1}{2} \int \vec{B} \cdot \vec{H} dv = \frac{1}{2} \int \frac{B^2}{\mu} A dx \quad (3-9)$$

When the springs are compressed a dx deformation, the iron slab also has a downward displacement dx . And by equation (3-9), we can obtain the changes in magnetic energy. As follows

$$dW_m = \frac{1}{2\mu} B^2 A dx \quad (3-10)$$

From the view of mechanical, we can know the magnetic energy exchange with mechanical energy as follows

$$dW = \hat{F} dx \quad (3-11)$$

If do not consider the leakage flux in the air. Therefore, the magnetic force \hat{F} is known by equation (3-10) and (3-11). We can obtain the magnetic force is



$$\hat{F} = \frac{1}{2\mu} B^2 A \quad (3-12)$$

From the relations of magnetomotive force, magnetic reluctance and magnetic flux density with Table 3.1. Obtain as follows.[14]

$$F = N \cdot i = \Phi \cdot R \quad (3-13a)$$

$$\Phi = \int_A \vec{B} \cdot d\vec{A} \quad (3-13b)$$

So we can rewrite the equation (3-12), by equation (3-13a), equation (3-13b), and obtain the magnetic force. The magnetic force has a relation with follows

$$\hat{F} = \frac{N^2 i^2}{2\mu A R^2} \quad (3-14)$$

So, we can calculate the magnetic force by the different magnetic reluctance and current, and use the magnetic force and spring force to control the bonding force.[11,15,16]

3.4 Bonding Force Control

In this thesis, we use the variable air gap to make the magnetic energy change between electromagnet and iron slab. And the magnetic reluctance is also different for the variable air gap. In the force control mechanism, we have a magnetic circuit, the path includes the electromagnet, air gap and iron slab as shown in Figure 3.3. And the air gap changes from 0 to 0.8mm for different experiments. In this thesis, we use papers to be air gap between electromagnet and iron slab, when the electromagnet attracts iron slab with each other. Papers make air gap between electromagnet and iron slab is fixed. So, by the variable air gap which we can see the difference for different air gap in the experiment. In the path of magnetic circuit, we must know the total magnetic reluctance by equation (3-7), then we can calculate the magnetic force by equation (3-14). When electromagnet attracts iron slab with each other, the springs also compressed by initial magnetic force. The initial magnetic force is larger enough to make the springs compressed. So, when we decrease the current of electromagnet step by step, the magnetic force will also less than spring force slowly. So bonding force is controlled by this principle.

3.4.1 Model of Force Control Mechanism

For force control mechanism, we can see its free state as Figure 3.4. And when we give an initial magnetic force make springs compressed, and Z-axis positioning lift up force control mechanism to bonding position. For this condition, we can simplify force control mechanism to a free body diagram as shown in Figure 3.5. Because we use papers to be air gap

between electromagnet and iron slab, and when we give an initial magnetic force, papers will also compress by this force. So, we must consider the effect of paper's compression. And we can obtain the balance equation as follows.

$$\frac{K_P}{n} X_c + K_S (X_S - nd) = \frac{N^2 i_0^2}{2\mu_0 A R_0^2(n)} \quad (3-15)$$

And we assume papers as a spring, and if $x > X_c$, the spring effect of paper will vanish. So we can know the spring constant of system is nonlinear in this model. By the equation (3-15) we can figure out, X_c is the compression of papers by magnetic force. As follows.

$$X_c = \frac{n}{K_P} \left(\frac{N^2 i_0^2}{2\mu_0 A R_0^2(n)} - K_S (X_S - nd) \right) \quad (3-16)$$

By the free body diagram of force control mechanism, we can obtain the equation with follows.

$$\begin{cases} \hat{F}(i_0) - \hat{F}(i) = (K_S + K_L + \frac{K_P}{n})x & x < X_c \\ \hat{F}(i_c) - \hat{F}(i) = (K_S + K_L)x & x \geq X_c \end{cases} \quad \text{when} \quad (3-17)$$

When the spring effect of papers vanishes, the current is called i_c . And we can figure out the relation with X_c , by equation(3-16), when $x < X_c$ as follows.

$$\hat{F}(i_c) = \hat{F}(i_0) - (K_S + K_L + \frac{K_P}{n})X_c \quad (3-18)$$

So, we can use the relation of equation (3-17) to rewrite the equation (3-16) as follows.

$$\left\{ \begin{array}{ll} \hat{F}(i_0) - \hat{F}(i) = (K_S + K_L + \frac{K_P}{n})x & x < X_c \\ \hat{F}(i_0) - \hat{F}(i) = (K_S + K_L)x + \frac{K_P}{n}X_c & x \geq X_c \end{array} \right. \text{when} \quad (3-19a)$$

And by the equation (3-14), we can know the magnetic reluctance vary with the displacement of iron slab and variable air gap. So we consider the two factors into the following equation.

$$\left\{ \begin{array}{ll} \frac{N^2}{2\mu_0 A} \left[\frac{i_0^2}{R_0^2(n)} - \frac{i^2}{(R_0(n) + \frac{x}{\mu_0 A})^2} \right] = (K_S + K_L + \frac{K_P}{n})x & x < X_c \\ \frac{N^2}{2\mu_0 A} \left[\frac{i_0^2}{R_0^2(n)} - \frac{i^2}{(R_0(n) + \frac{x}{\mu_0 A})^2} \right] = (K_S + K_L)x + \frac{K_P}{n}X_c & x \geq X_c \end{array} \right. \text{when} \quad (3-19b)$$

where

$$R_0(n) = R_{core} + R_{iron} + R_{shell} + R_{airgap} \quad (3-20)$$

And $R_0(n)$ is the magnetic reluctance in magnetic circuit for different air gap.

When $n > 4$, we assume the displacement of iron slab is small enough, and ignore its effect on magnetic reluctance.

$$\text{when } n > 4, R_0(n) + \frac{x}{\mu_0 A} \rightarrow R_0(n) \quad (3-21)$$

Now, we can simplify equation (3-19b) for $n > 4$ as follows

$$\hat{F}_i = \hat{F}_0 - \hat{K}x \quad (3-22)$$

Where,

$$\hat{F}_i = i^2 \quad (3-23a)$$

$$\hat{K} = \begin{cases} \frac{2\mu_0 A}{N^2} R_0^2(n) (K_S + K_L + \frac{K_P}{n}) & x < X_c \\ \frac{2\mu_0 A}{N^2} R_0^2(n) (K_S + K_L) & x \geq X_c \end{cases} \quad \text{when} \quad (3-23b)$$

$$\hat{F}_0 = \begin{cases} i_0^2 & x < X_c \\ i_0^2 - \frac{2\mu_0 A}{N^2} R_0^2(n) \frac{K_P}{n} X_c & x \geq X_c \end{cases} \quad \text{when} \quad (3-23c)$$

By the equation (3-22), we calculate the displacement of iron slab by computer. And we can know in our model, $K_L x$ is the value of load cell, that is, the bonding force. So after calculating the displacement of iron slab, we can plot the curve of bonding force by computer. And compare with experiment.

3.5 Experiment Result

In the experiment, we change the air gap; i.e. thickness of papers, between iron slab and electromagnet. And by the equation (3-22), we can know the displacement divided into two stages. Figure 3.6 to Figure 3.14 show the experiment result and theoretical curve from 0mm to 0.8mm of air gap. From theoretical curve, we can see the turning point obvious at the current that equals to i_c . And we could see the theoretical curve do not match with experiment curve for $n=0$ to $n=4$. We think the effects of residual magnetism and hysteresis make experiment do not match with

theoretical curve. Especially, for $n=0$ experiment curve is affected obvious by the effects residual magnetism and hysteresis. But for $n=5$ to $n=8$, the effects of residual magnetism and hysteresis do not affect the experiment result obvious. For $n=7$ and $n=8$, the bonding force output is more smoothly and the slope of experiment curve also smaller than the others, this could make us to control bonding force more easily. The reason for the smaller slope and easy to control, is the greater air gap, and the magnetic reluctance also greater to make the experiment curve more smoothly. But in this thesis, the initial current which we set is 0.12A, and the maximum air gap is 0.8mm. If the air gap set up to 0.9mm and the initial current is also 0.12A, the initial magnetic force of electromagnet will not large enough to attract iron slab with each other. So if we want to set larger initial current, we must make the air gap greater than before, and find the appropriate air gap make the curve of output force smoothly. Otherwise, the experiment curve will affected by residual magnetism and hysteresis, as shown in Figure 3.15.

Chapter 4 Hardware and Software Introduction

When design a mechanism, we must know our need then we could find the matched hardware. In this mechanism most important elements of Z-axis position and force control of two parts. The servomotor provides power to drive the force control platform upward. The electromagnet and permanent magnet provide repulsive force to push the substrate up and contact with chip. So the following are the introduction of hardware.

4.1 D.C. Servomotor

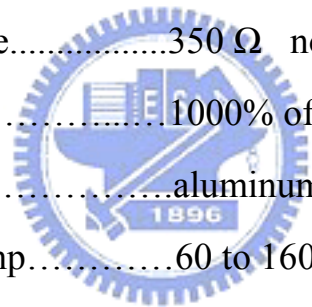
The motor we chose in the system as actuator is SmartMotor 2315D. Traditionally, an entire servomotor system includes: encoder, motion controller, driver, servomotor and cables etc. The SmartMotor integrates these components in a single module, and it becomes an integrated servo system. It includes a very high quality, high performance brush-less D.C. servomotor which has a rotor with extremely powerful rare earth magnets and a stator that is a densely wound multi-slotted electromagnet. There are seven I/O channel available on a SmartMotor 2315D. They can be assigned as inputs, outputs, or 10 bits analog inputs individually. Besides, there is also an encoder which resolution is 2000 counts/revolution coupled to the motor shafts to provide feedback signals for the position feedback loops. The servomotor works with a D.C. power supplied 24 volts and its communication are under the RS232 interface. The major advantage for our selection is volume reduction. With all components integrating in a single servomotor module, we can efficiently reduce system volume.[4]The SmartMotor is shown in Figure 4.1.

4.2 Load Cell

Load cell in the force control mechanism is important to measure the contact force. The load cell needs accuracy and sensitive. The load cell we chose is FUTEK S-BEAM 10lb shown in Figure 4.2.

Its features and performance show as follows.

- Rated Output (RO).....2 mV/V
- Nonlinearity..... $\pm 0.1\%$ RO
- Hysteresis..... $\pm 0.1\%$ RO
- Operating Temp.....-60 to 200°F
- Excitation (Max).....10 VDC
- Bridge Resistance.....350 Ω nom
- Safe Overload.....1000% of RO
- Material.....aluminum
- Compensated temp.....60 to 160°F
- Weight.....9g



4.3 SMI Motor Control Software

When you open the SMI software, SmartMotor Playground will show on your monitor, it provides users with real-time operation of motors. You can change the parameters, or human interface setup and you can instantly see the results. In SmartMotor Playground below the screen there is a 'Show SMI' button, it will then go after the implementation of the SMI II standard control interface. As shown in Figure 4.3. The Configuration:

through automatic search, the state of this column can be connected to a computer that all the motor situation. Second, Terminal: this window enables users through immediate and direct instructions motor control. Third, Program editor: this window allows users to edit programs motors, and transmission.

4.4 NI USB-6229 Multifunction DAQ

The National Instruments USB-6229 is a USB high-performance M Series multifunction data acquisition (DAQ) module optimized for superior accuracy at fast sampling rates. As shown in Figure 4.4. The NI USB-6229 is ideal for applications such as data logging and for sensor measurements when used with NI signal conditioning. The USB-6229 is designed specifically for mobile or space-constrained applications. Plug-and-play installation minimizes configuration and setup time, while direct screw-terminal connectivity helps keep costs down and simplifies signal connections. This USB-6229 also features the new NI Signal Streaming technology, which provides DMA-like bidirectional high-speed streaming of data across the USB bus. USB-6229 is shown in Figure 4.4

- 32 analog inputs (16-bit, 250 kS/s).
- 4 analog outputs (16-bit, 833 kS/s), 48 digital I/O (32 at up to 1MHz), and 32-bit counters.
- NI Signal Streaming for sustained high-speed data streams over USB.
- Compatible with LabVIEW, LabWindows/CVI, and Measurement Studio for Visual Studio .NET.

Chapter 5 Conclusion

The main purpose of this thesis is to design the z-axis vertical positioning system and bonding force control of flip chip devices. For this purpose, we replace pneumatic cylinder with electromagnet and springs to control the bonding force. And from the experiment result, we can know that use magnetic force to control bonding force is available. The resolution of force control can also meet the current requirements, and it is also solve the problem of stick-slip effect. And z-axis vertical positioning, uses DC servomotor with ball screw and linear slider to positioning the platform in the flip-chip process. The z-axis vertical positioning is closed loop control. By the inner encoder of DC servomotor, we can use it to make positioning more precise, and reduce the positioning errors. Although our force control and z-axis positioning mechanism have many advantages, there are still some flaws. In the future, we will improve the z-axis positioning and force control mechanisms.

References

- [1] 李篤誠 The development strategy of Taiwan dicing saw industry 台灣切割機產業的發展策略
- [2] 謝新協, An Integration study of SMD LED pick and place Machine 「表面黏著型發光二極體取放機構之研製」, 私立中原大學, 碩士論文, 91年
- [3] 江榮富, Investigation of Servo Control for High Accuracy Positioning 「伺服精密定位控制之探討」, 私立中原大學, 碩士論文, 90年
- [4] 張淦堯, 「機載雷達偵照系統之視線控制」, 碩士論文, 國立交通大學機械工程學系, 95年。
- [5] 洪敬堯, 「DSP-Based 之即時多工運動控制器研製」, 碩士論文, 國立交通大學機械工程研究所, 94年。
- [6] 井澤 實, 「精密定位技術及其設計技術」, 建宏書局, 1992。
- [7] 洪榮哲編譯, 「機構設計精密定位法」, 全華書局, 1998。
- [8] 楊憲東, 「精密機械控制原理與模擬」, 全華圖書, 民國八十七年。
- [9] Sonja Macfarlane, Elizabeth A. Croft, "Jerk-Bounded Manipulator Trajectory Planning: Design for Real-Time Applications." IEEE Trans.

Robot. Automat., vol.19, no.1, pp.42-52, 2003.

- [10] 施禕迪，「直線馬達運動平台之高精密度控制含摩擦力補償」，博士論文，國立交通大學機械研究所，93年。
- [11] 溫坤禮，曹建祈，「工程電磁學」，新文京開發出版股份有限公司，。
- [12] 王以真，「實用磁路設計」，全華圖書，84年。
- [13] David K. Chen, “Field and Wav Electromagnetic”，Addison Wesley, 1989, USA.
- [14] 鄒應嶼，「伺服系統設計」，課程講義，電力電子與運控制實驗室，1994。
- [15] 黃忠良，「磁懸浮與磁力軸承-磁力懸浮系統工程及磁力軸承技術」，復漢出版社，1999.
- [16] 林坤森，「電磁動力式激震器之設計與應用」，碩士論文，國立交通大學機械工程學系，91年。
- [17] A. Bossavit, “Computational Electromagnetism”，Academic Press Ltd.,New York ,1998.

Figures

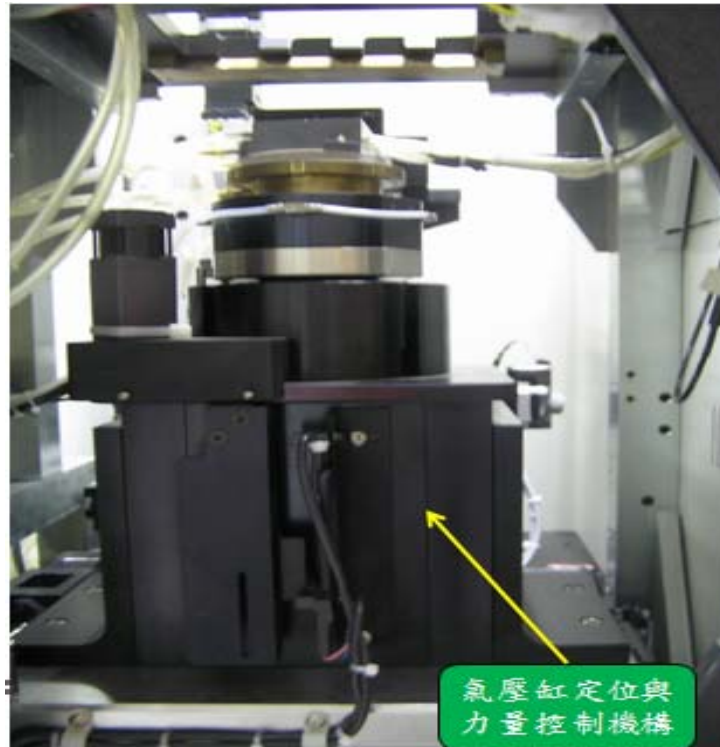


Figure 1.1 Pneumatic cylinder positioning system.

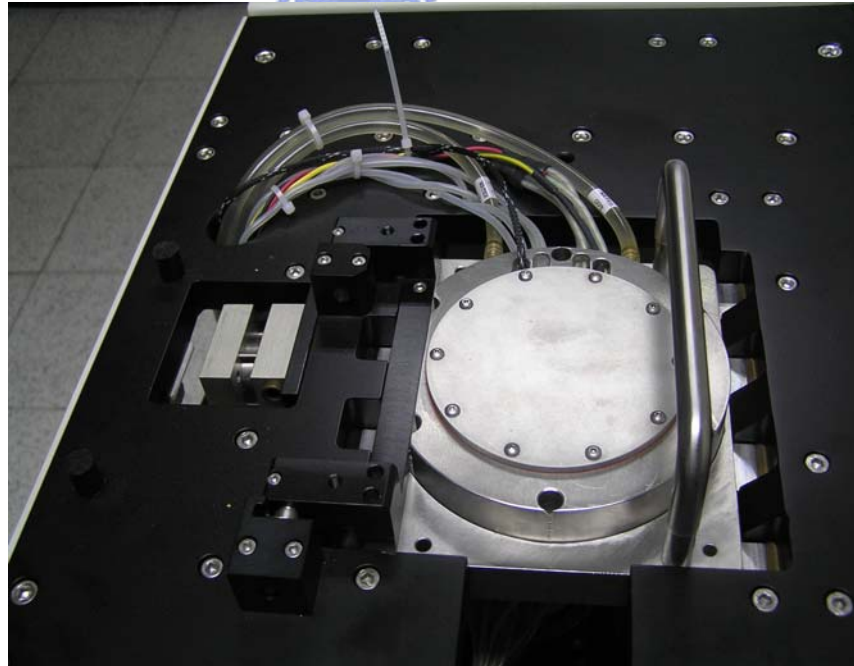


Figure 1.2 Lid closed

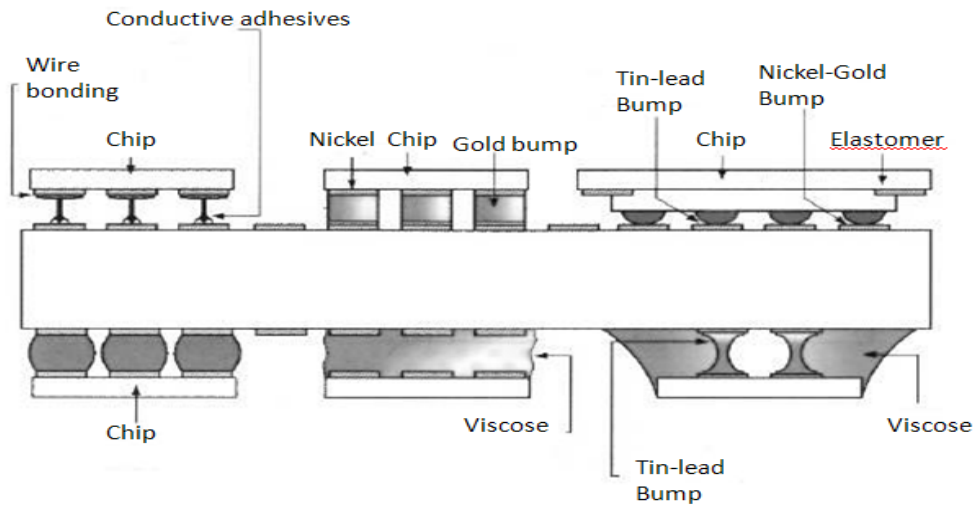


Figure 1.3 Six kinds of flip chip

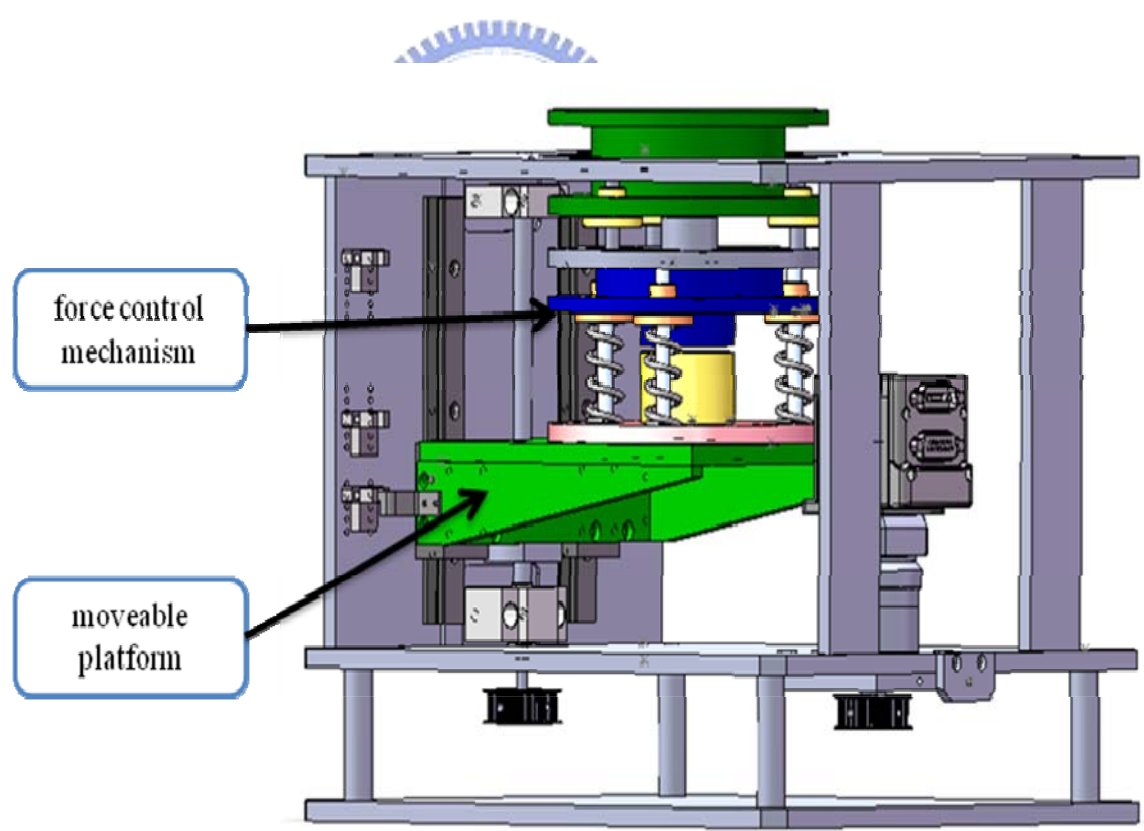


Figure 2.1 Conceptual mechanism

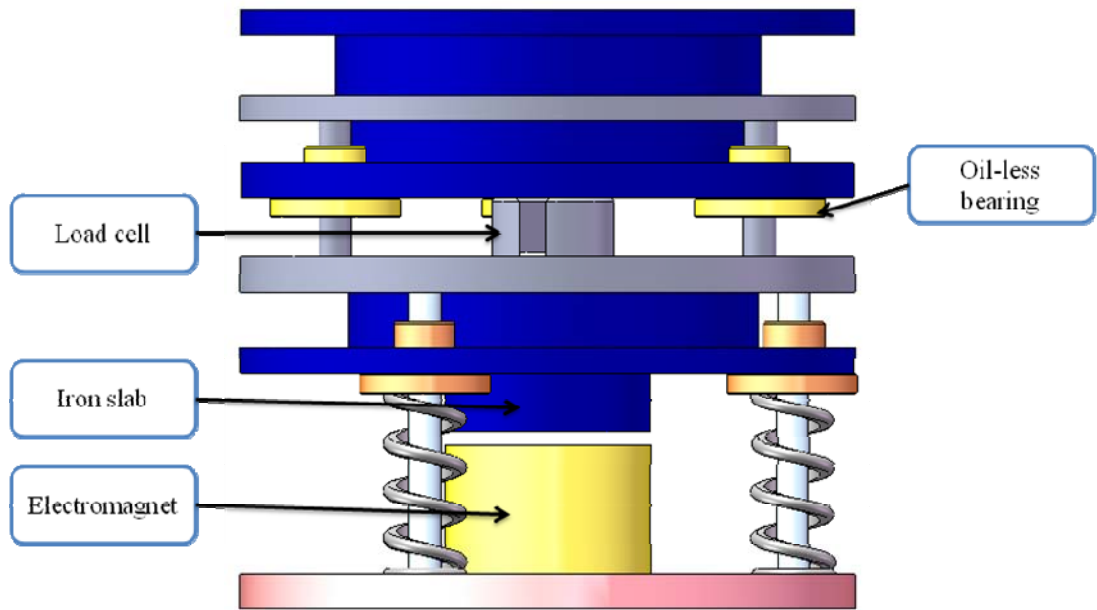


Figure 2.2 conceptual force control mechanism

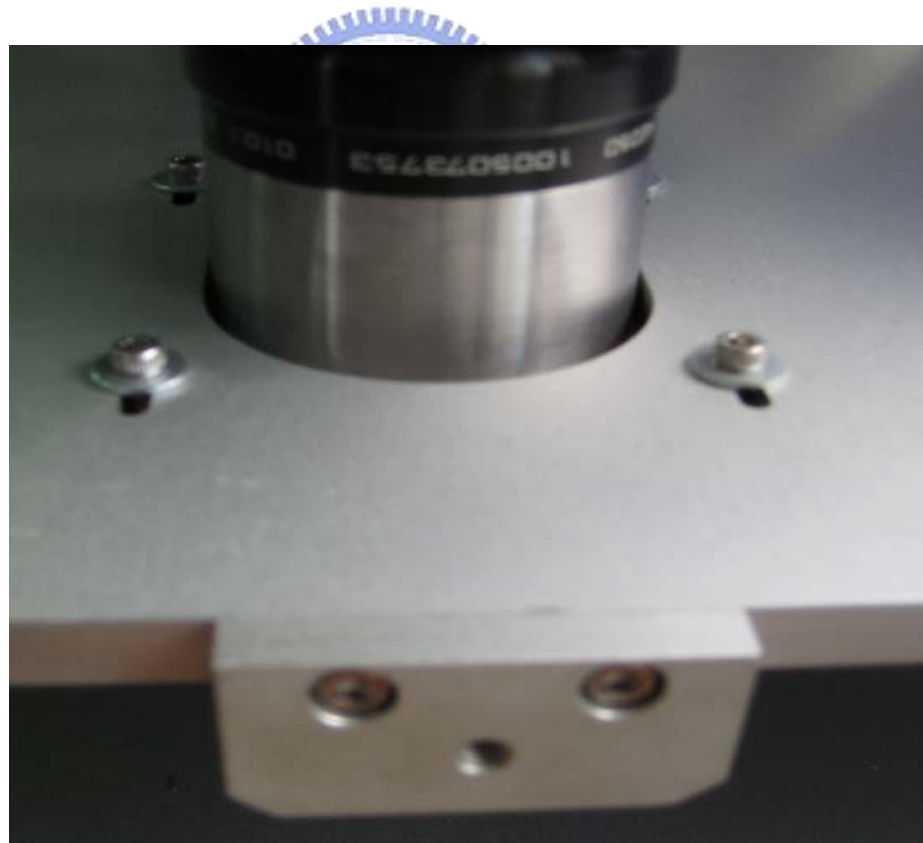


Figure 2.3 Fixed base and the four long-axis holes.

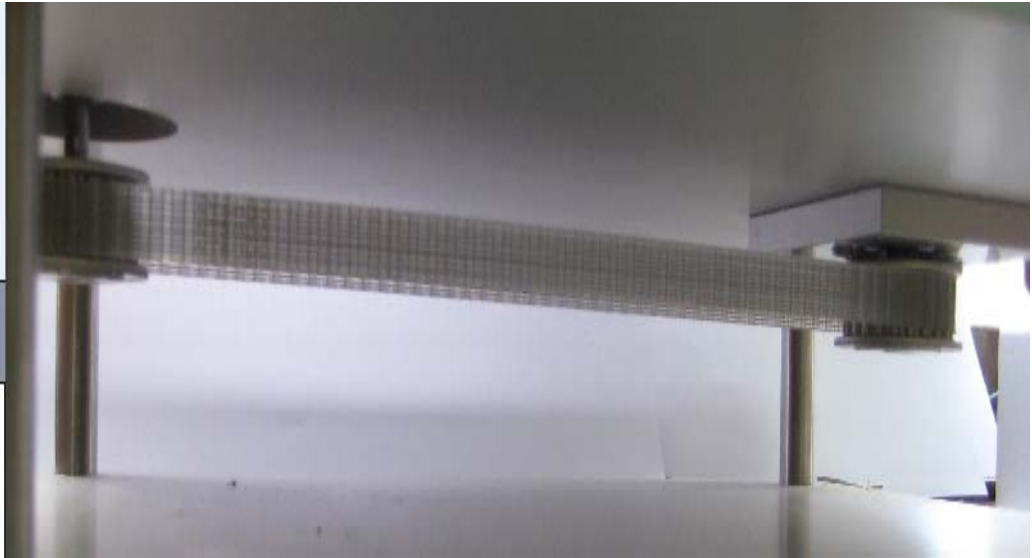


Figure 2.4 Timing pulley and timing belt.

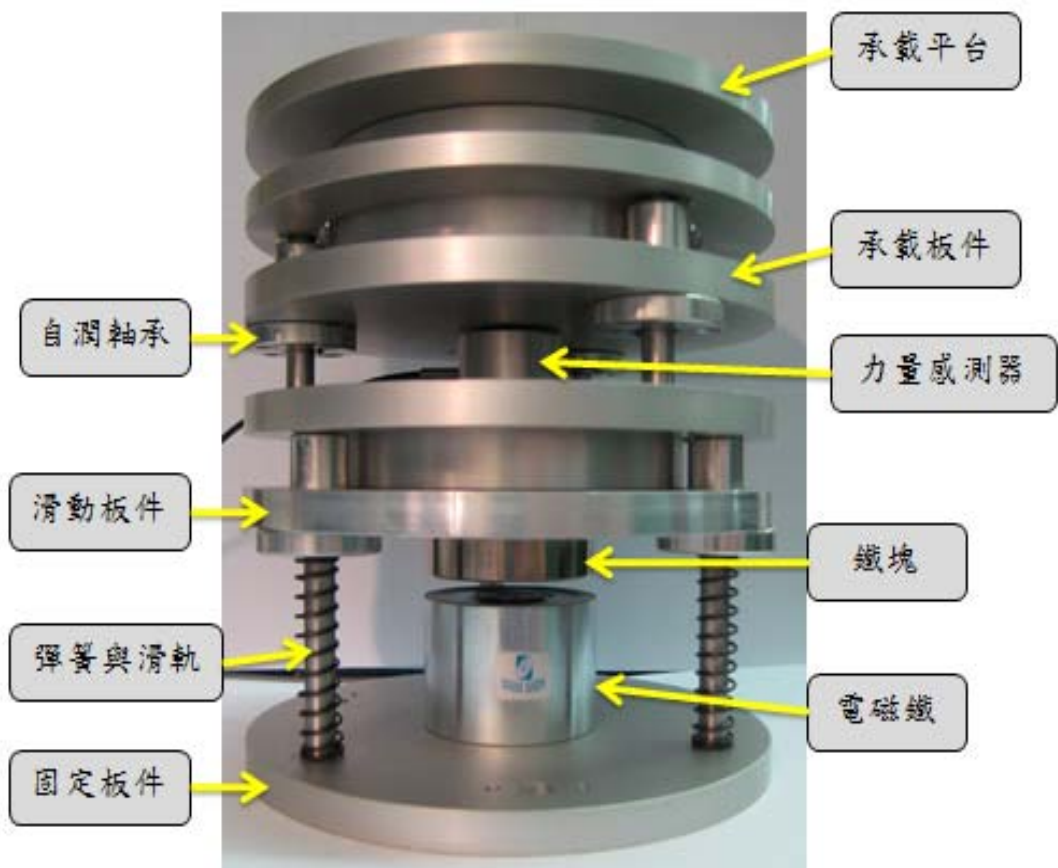


Figure 2.5 Force control mechanism.

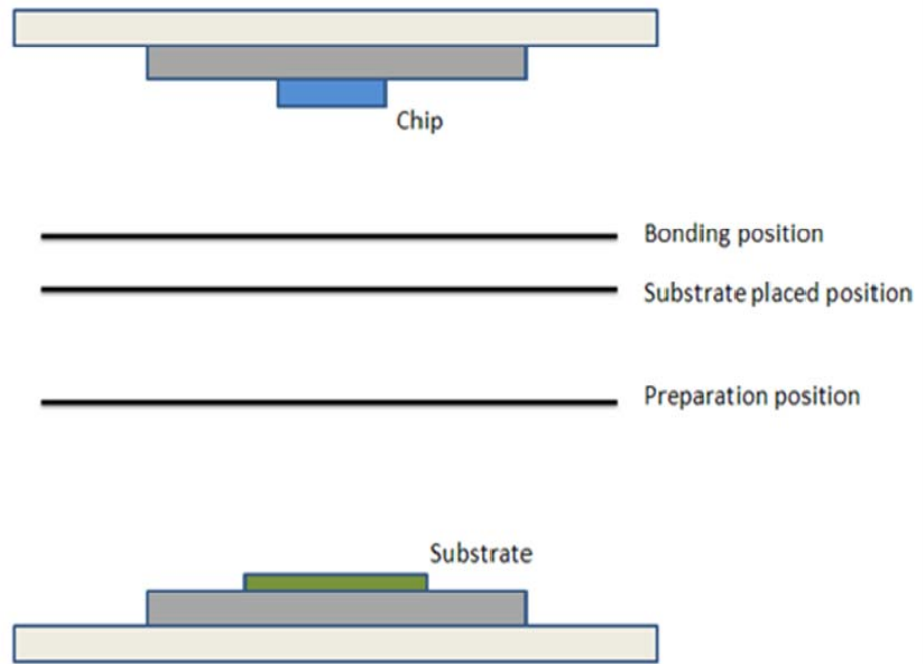


Figure 2.6 Relationship of position

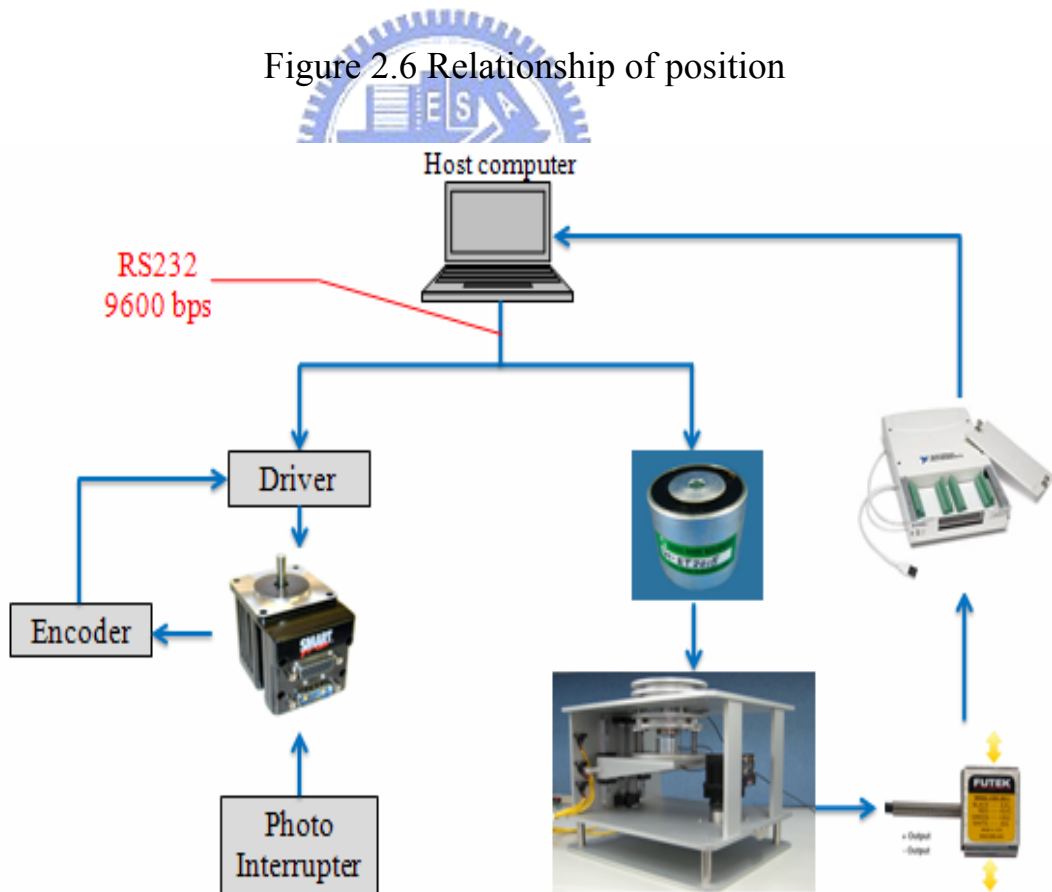


Figure 2.7 The control system architecture.

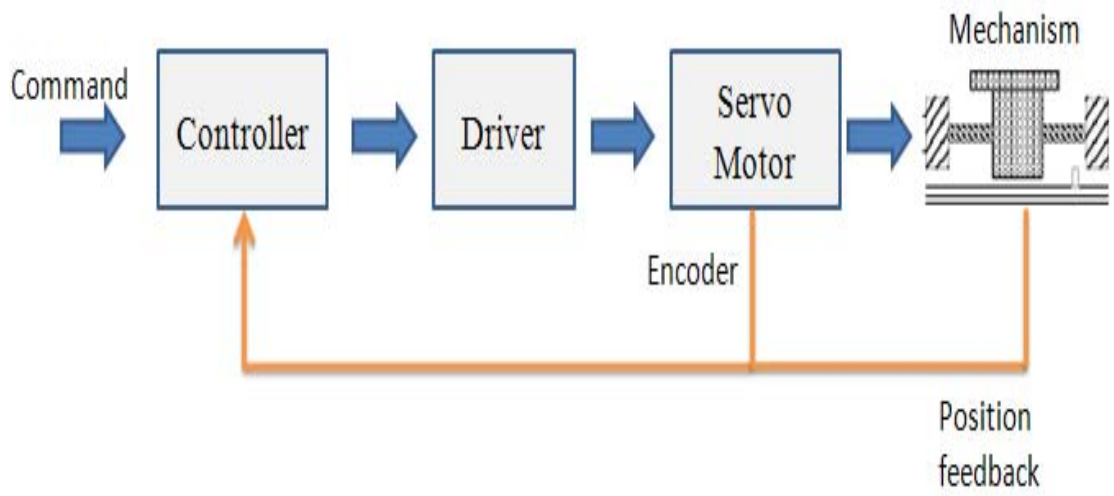


Figure 2.8 Servomotor close loop control

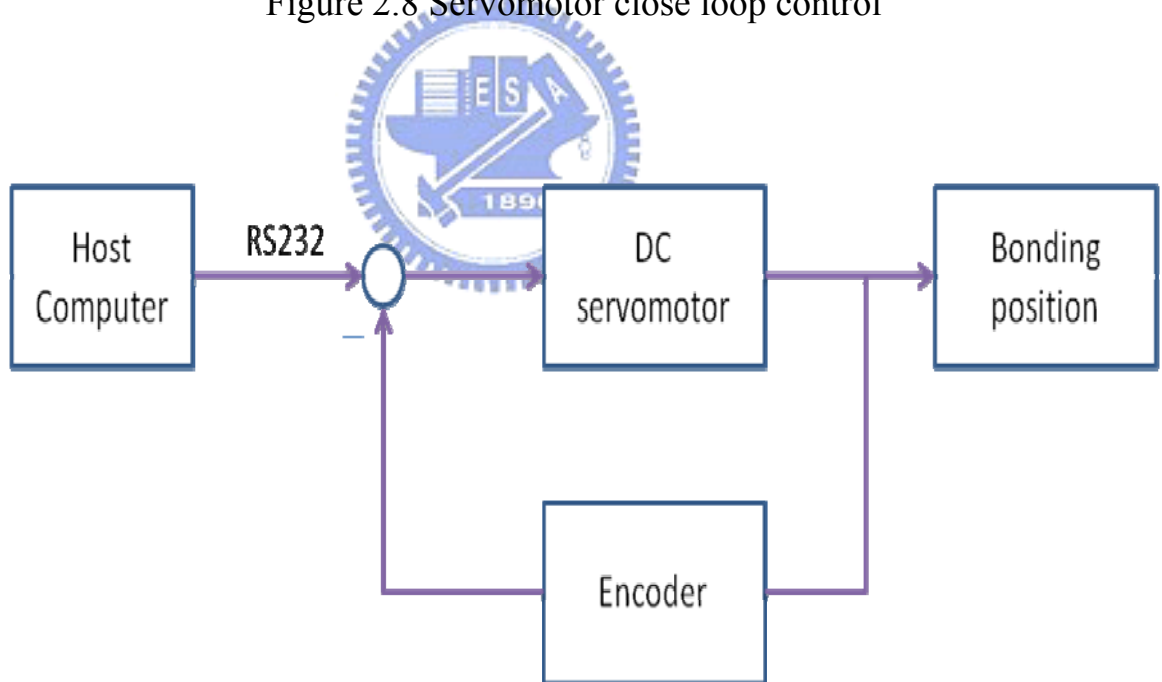


Figure 2.9 First stage positioning control block diagram.

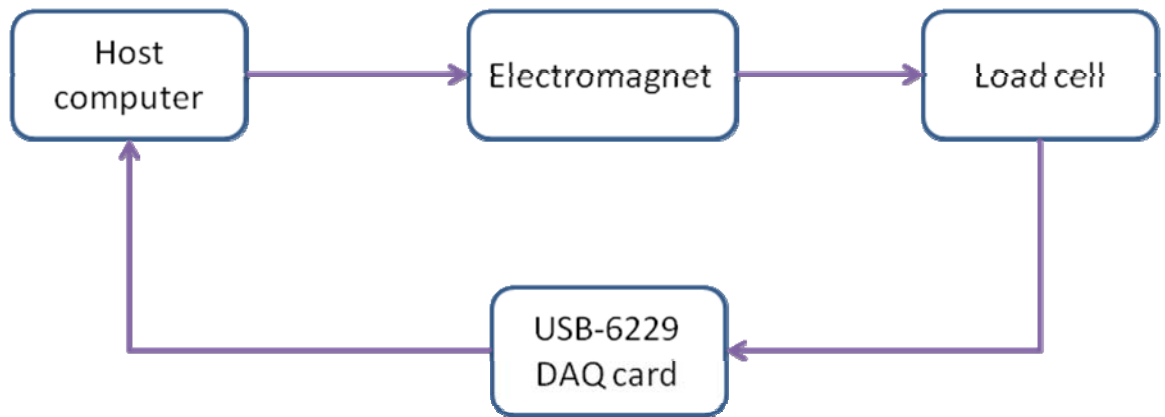


Figure 2.10 Force control architecture.

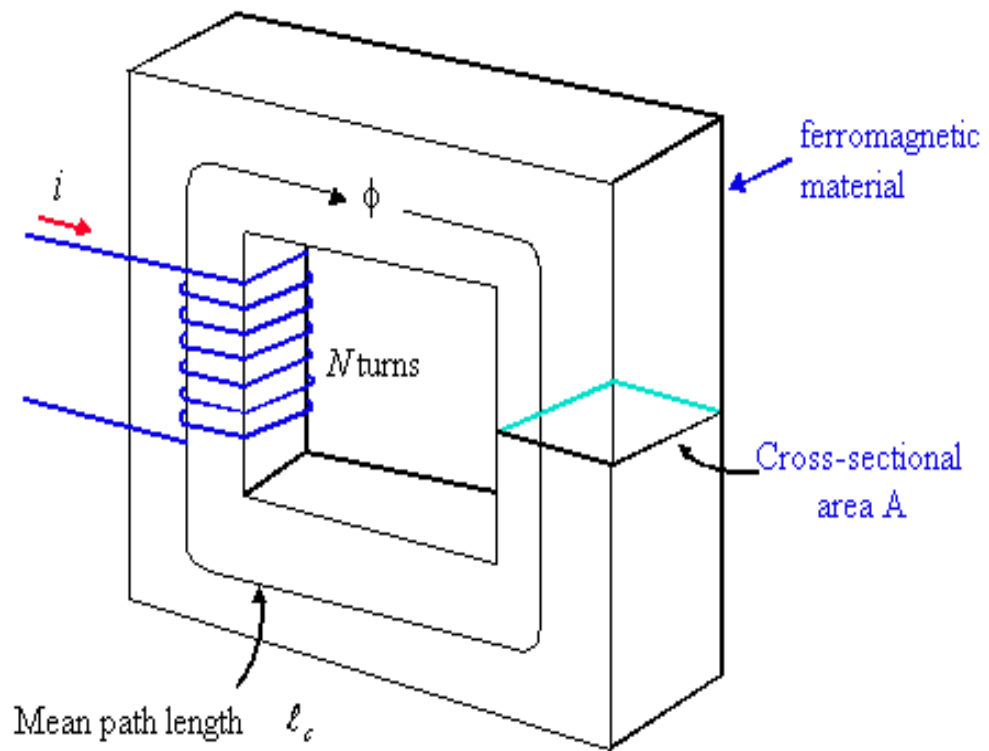


Figure 3.1 Coil around the square core.

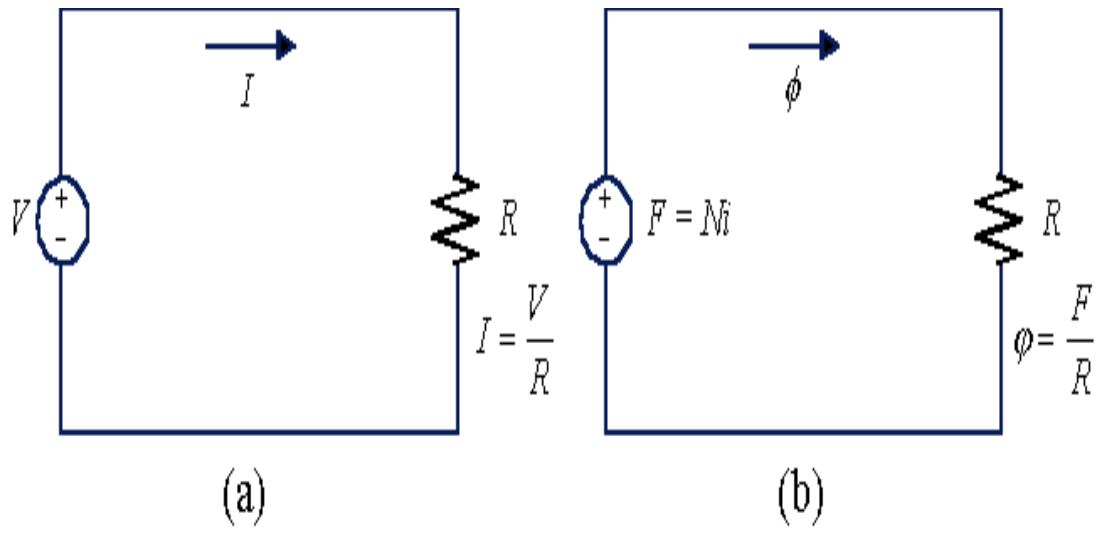


Figure 3.2 Similarities of circuit and magnetic circuit.

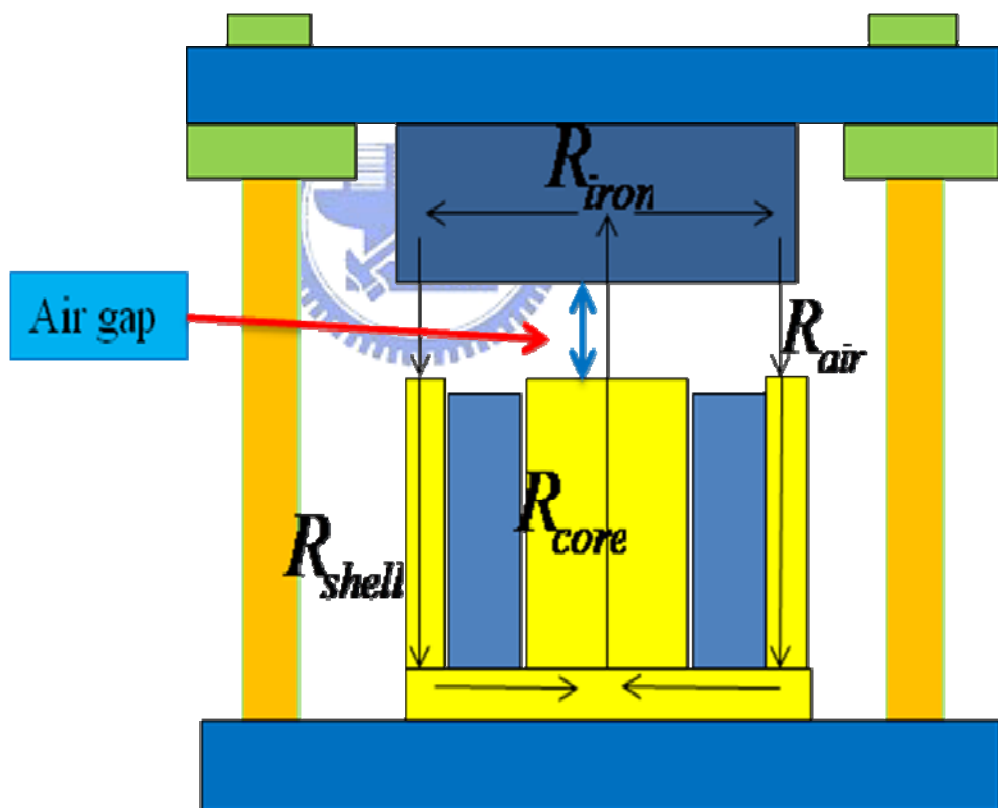


Figure 3.3 magnetic circuit of force control mechanism.

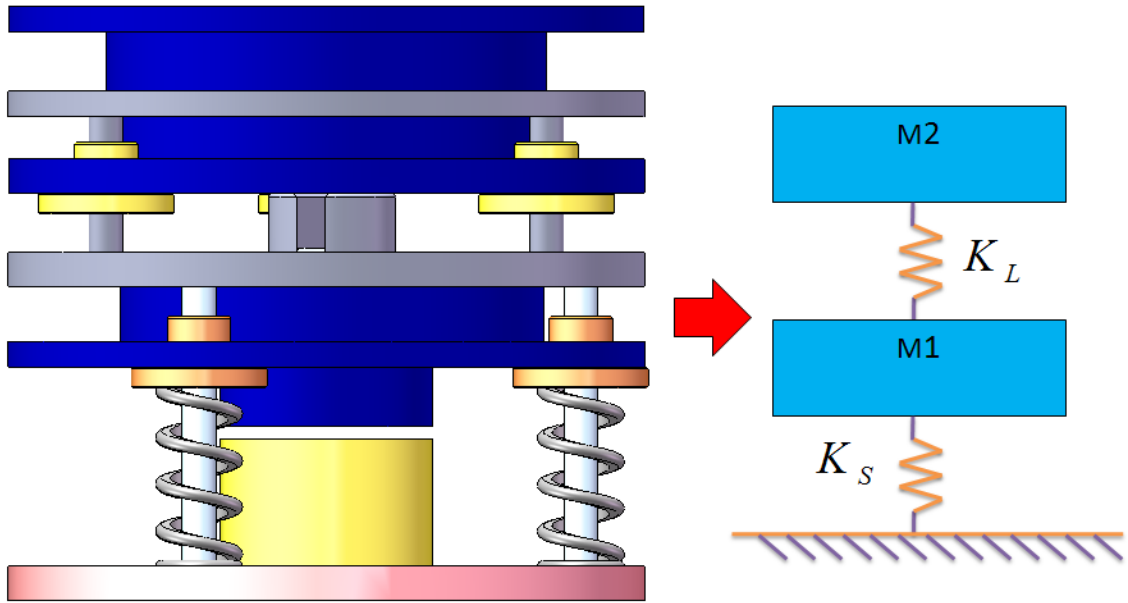


Figure 3.4 Free state of force control mechanism

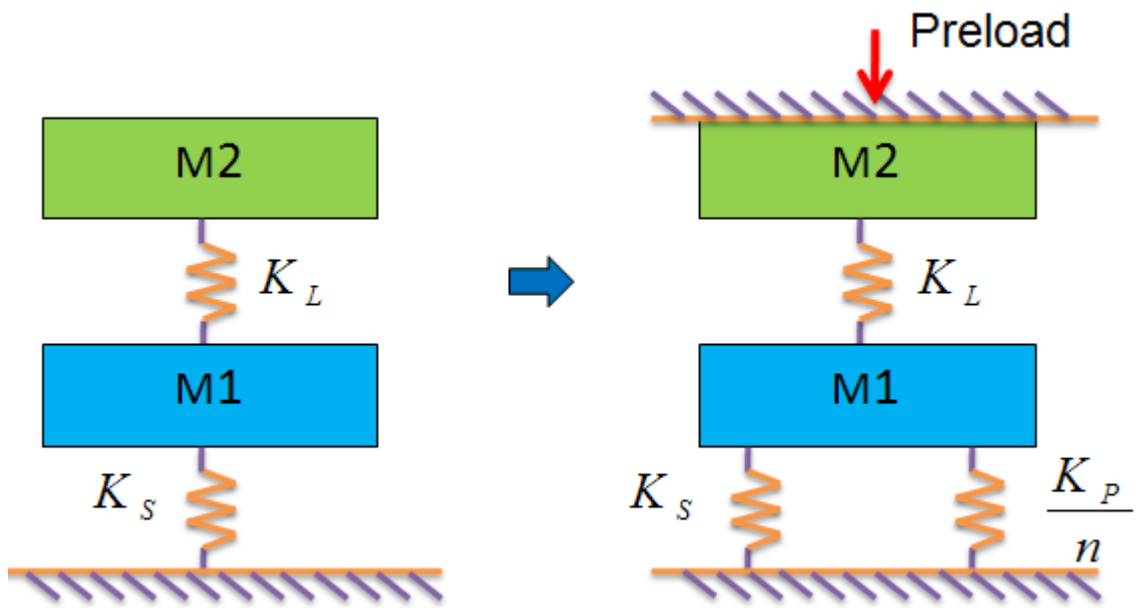


Figure 3.5 The free body diagram of force control mechanism, when it is lifted up to bonding position.

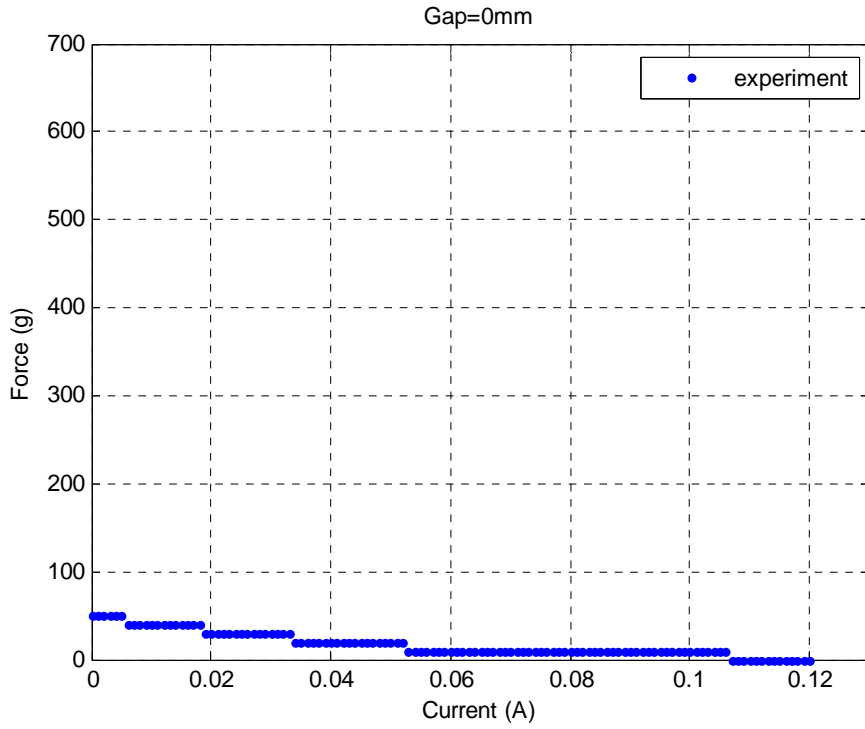


Figure 3.6 Air gap =0mm, current=0.12A

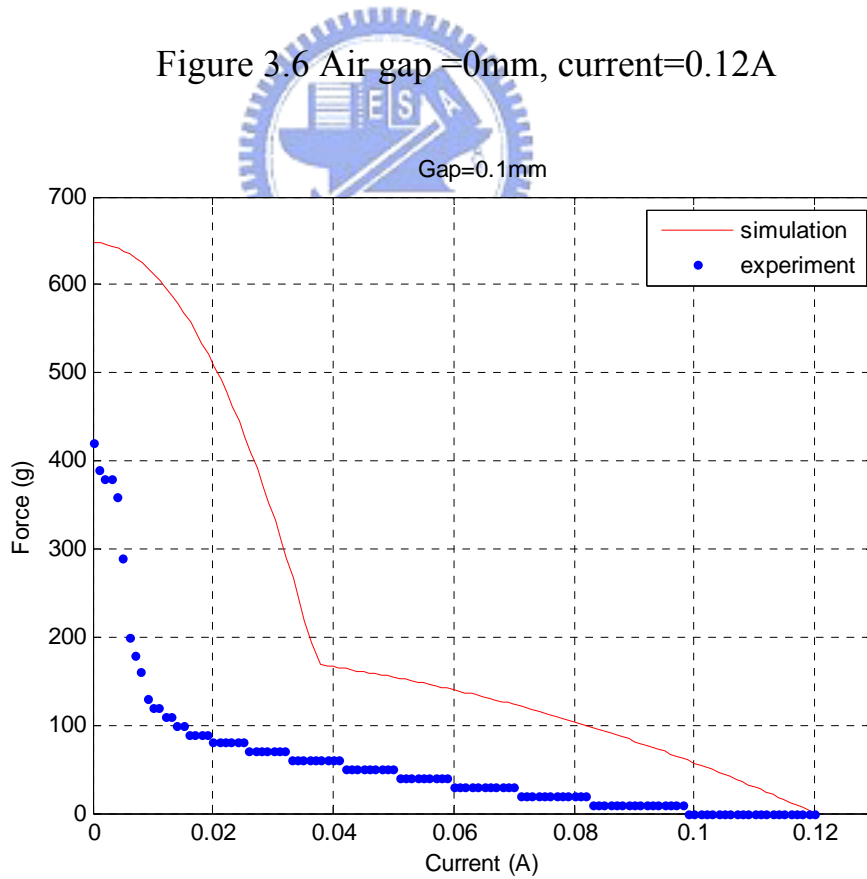


Figure 3.7 Air gap =0.1mm, current=0.12A.

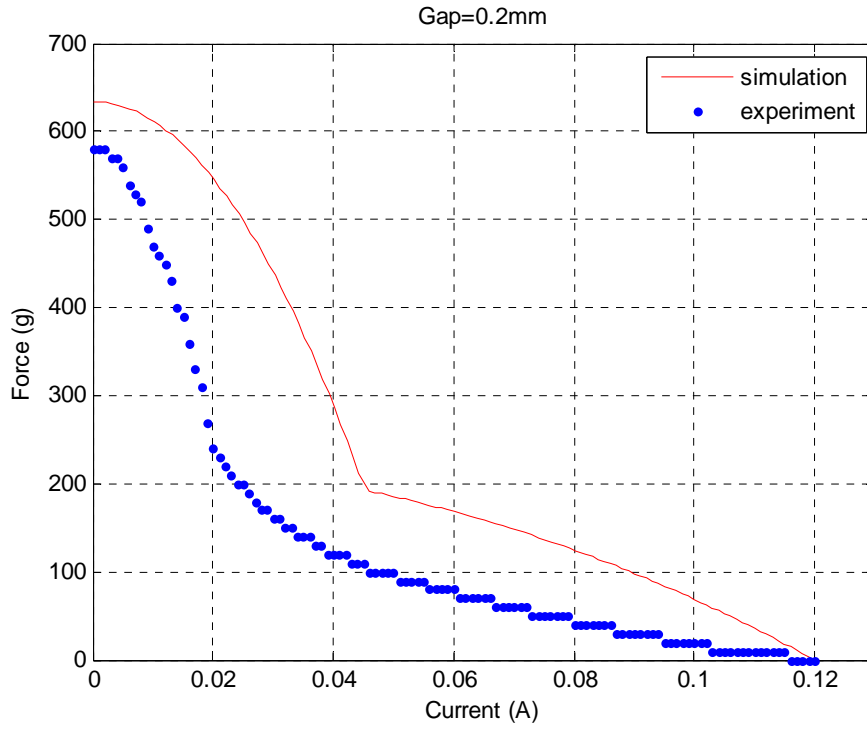


Figure 3.8 Air gap =0.2mm, current=0.12A.

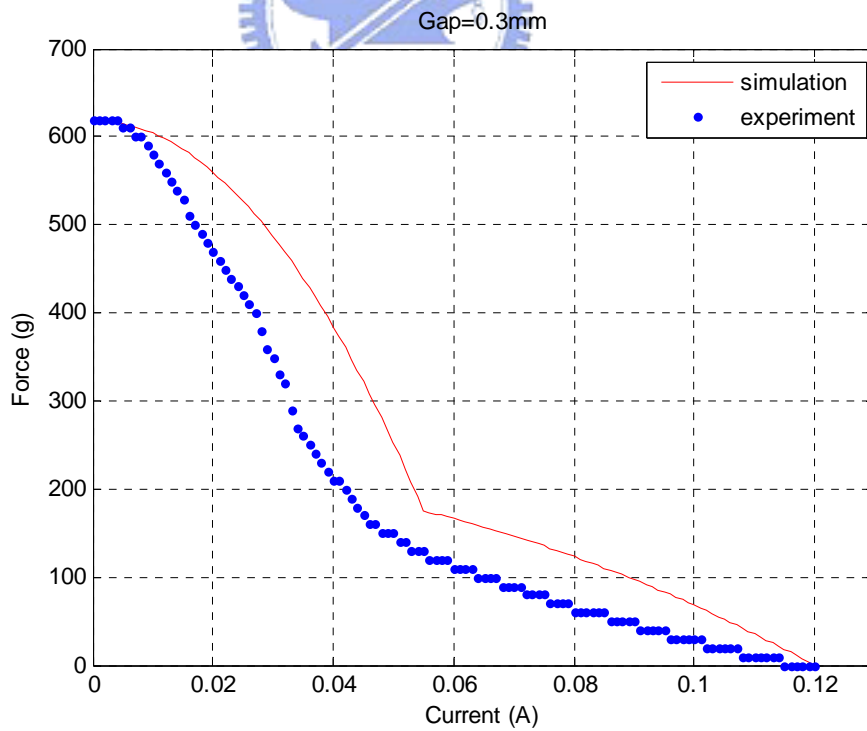


Figure 3.9 Air gap=0.3mm, current=0.12A.

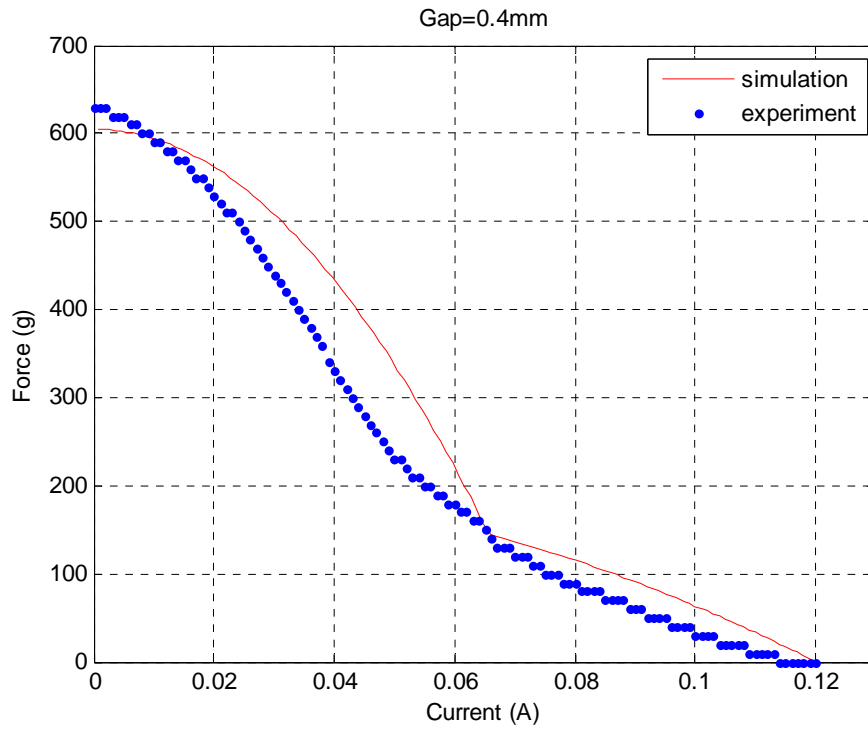


Figure 3.10 Air gap =0.4 mm, current=0.12A

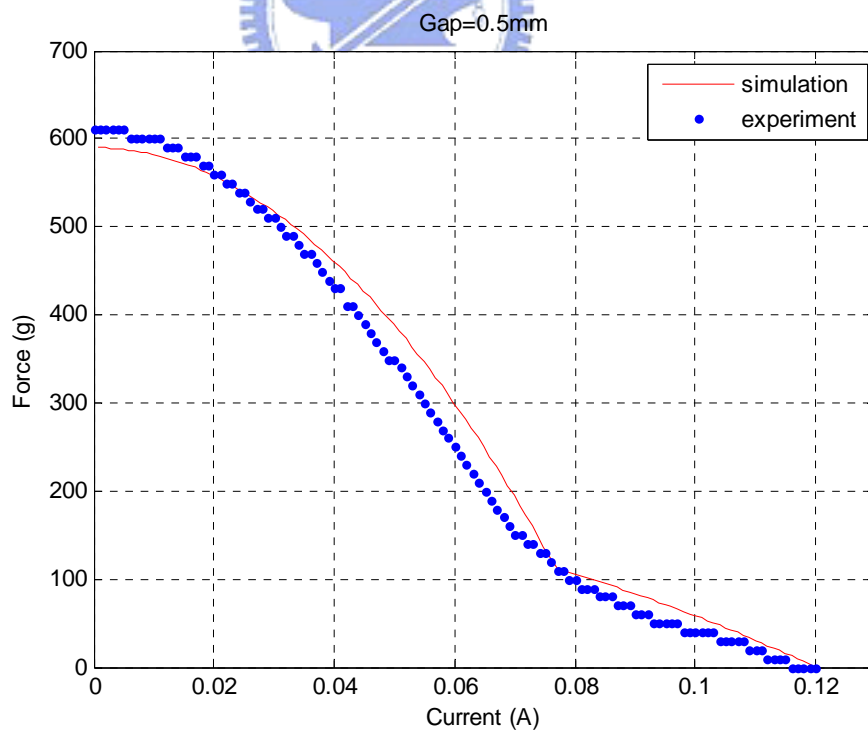


Figure 3.11 Air gap =0.5 mm, current=0.12A

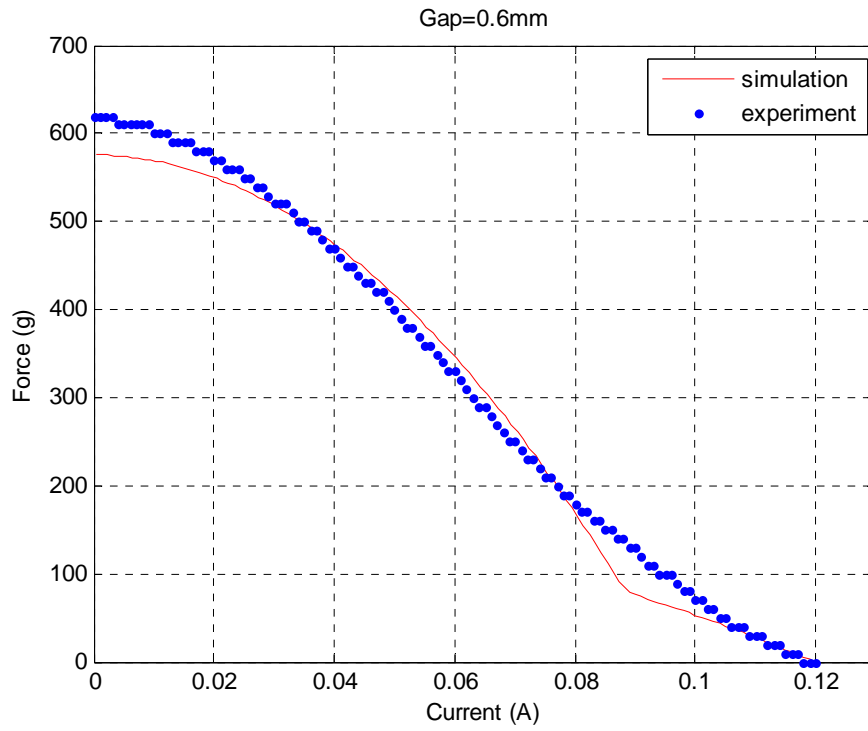


Figure 3.12 Air gap =0.6 mm, current=0.12A

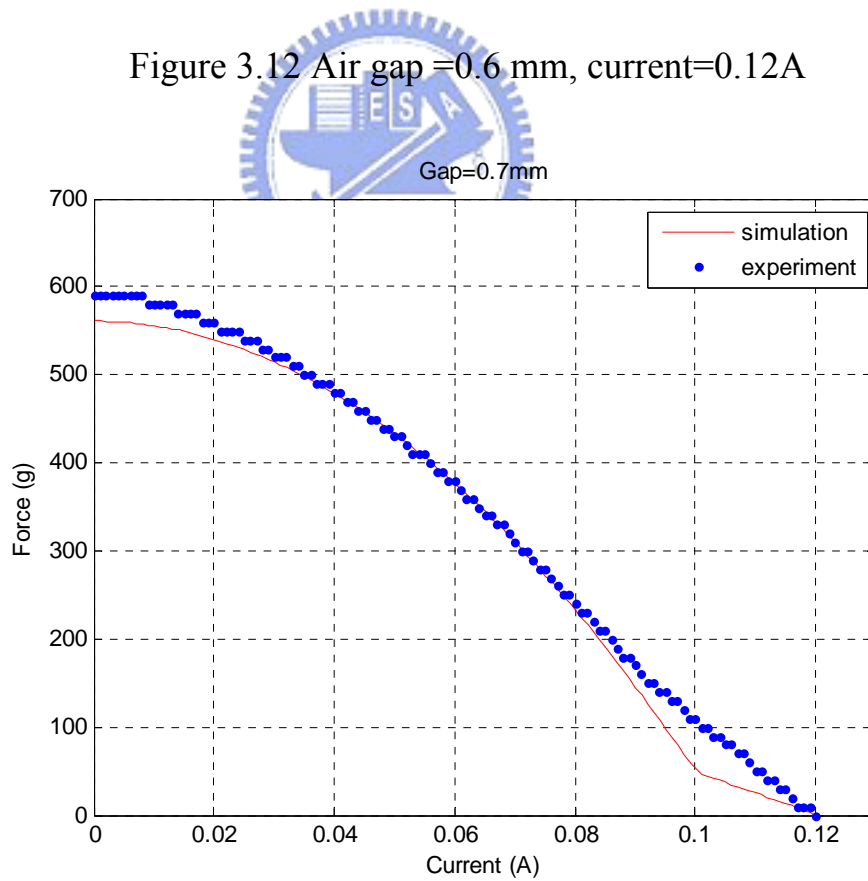


Figure 3.13 Air gap =0.7 mm, current=0.12A

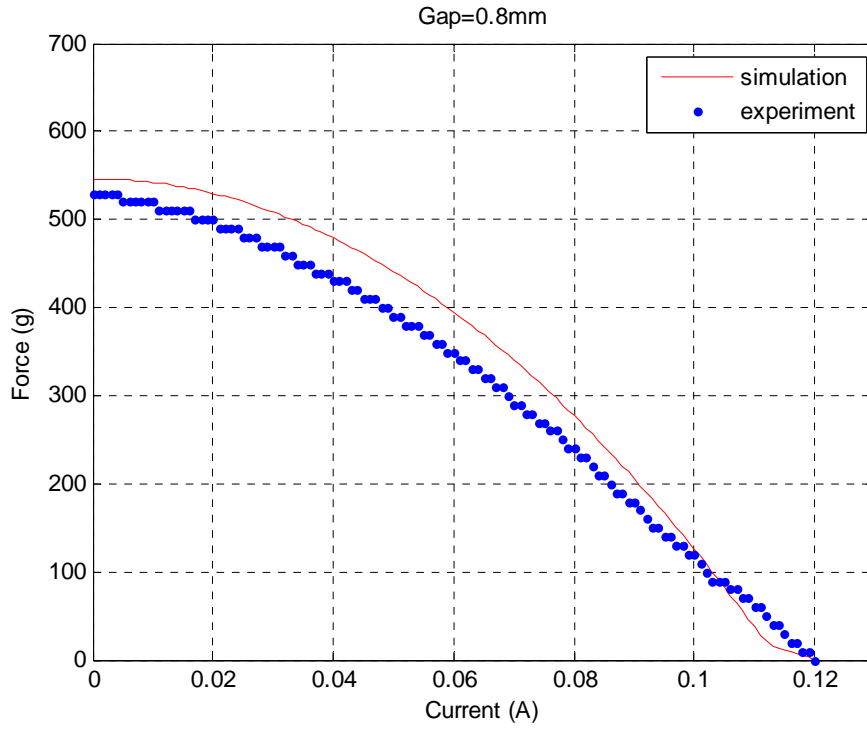


Figure 3.14 Air gap =0.8 mm, current=0.12A

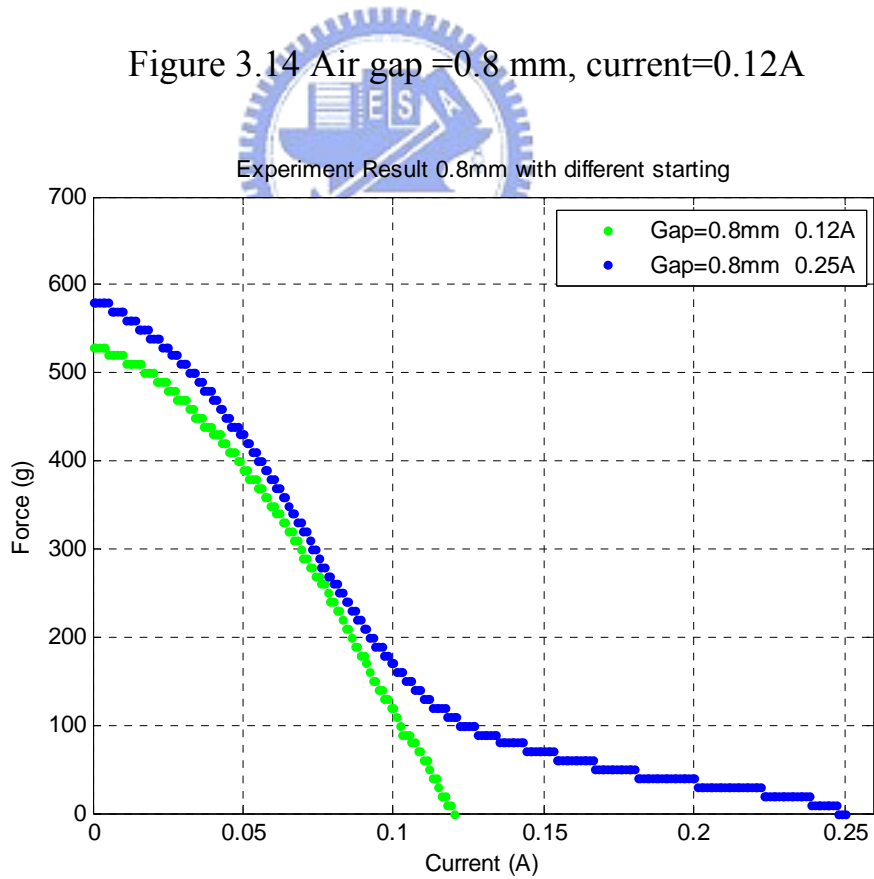


Figure 3.15 Air gap=0.8mm,current=0.25A.



Figure 4.1 SmartMotor 2315D

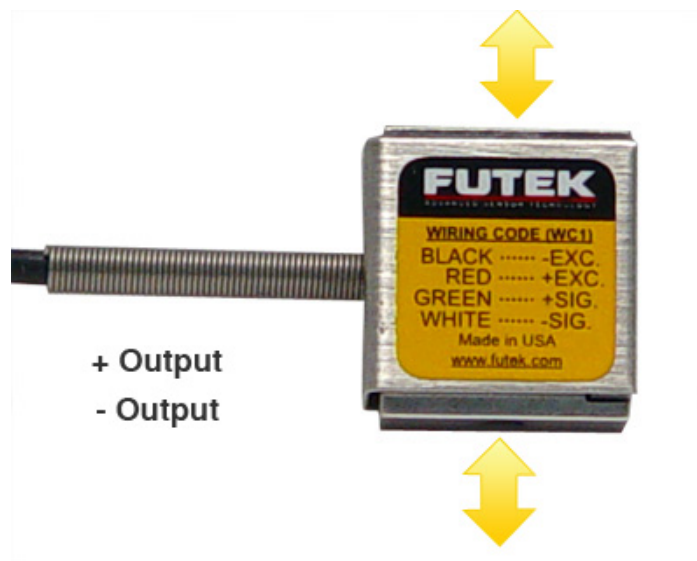


Figure4.2 FUTEK LSB200 10lb.

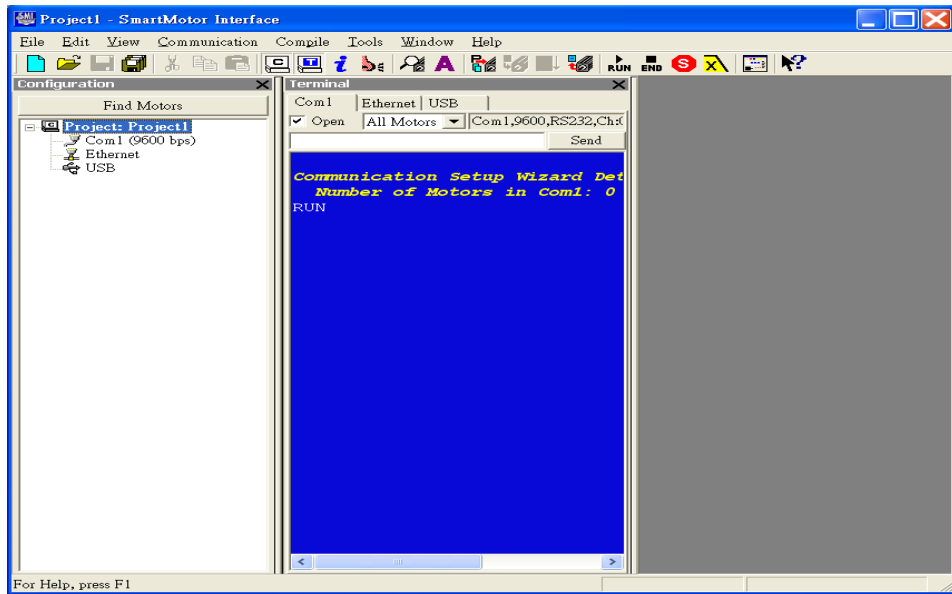


Figure 4.3 SMI software.



Figure 4.4 NI USB-6229 DAQ card.

Table

Circuit	Magnetic circuit
$E=IR$	$F=\Phi R=Ni$
$J=I/A$	$B=\Phi/A$
導電係數 $\sigma=1/\rho$	導磁係數 μ
$R=\rho\frac{l}{A}$	$R=\frac{l}{\mu A}$
$\sum E=\sum IR$	$\sum F=\sum Hl_c$

Table 3.1 Duality of circuit and magnetic circuit.

